J Appl Physiol
90: 593–600, 2001.

Cerebral gas embolism absorption during hyperbaric therapy: theory

ANNETTE B. BRANGER,[1] CHRISTIAN J. LAMBERTSEN,[2] AND DAVID M. ECKMANN[3]
[1]*Department of Biomedical Engineering, Northwestern University, Evanston, Illinois 60208;*
[2]*Institute for Environmental Medicine and* [3]*Department of Anesthesia and Institute for Medicine and Engineering, University of Pennsylvania, Philadelphia, Pennsylvania 19104*

Received 18 February 2000; accepted in final form 1 September 2000

Branger, Annette B., Christian J. Lambertsen, and David M. Eckmann. Cerebral gas embolism absorption during hyperbaric therapy: theory. *J Appl Physiol* 90: 593–600, 2001.—Cerebral gas embolism is a serious consequence of diving. It is associated with decompression sickness and is assumed to cause severe neurological dysfunction. A mathematical model previously developed to calculate embolism absorption time based on in vivo bubble geometry is used in which various conditions of hyperbaric therapy are considered. Effects of varying external pressure and inert gas concentrations in the breathing mixtures, according to US Navy and Royal Navy diving treatment tables, are predicted. Recompression alone is calculated to reduce absorption times of a 50-nl bubble by up to 98% over the untreated case. Lowering the inhaled inert gas concentration from 67.5% to 50% reduces absorption time by 37% at a given pressure. Bubbles formed after diving and decompression with He are calculated to absorb up to 73% faster than bubbles created after diving and decompression with air, regardless of the recompression gas breathed. This model is a useful alternative to impractical clinical trials in assessing which initial step in hyperbaric therapy is most effective in eliminating cerebral gas embolisms should they occur.

decompression sickness; diffusion; multiple gas model; in vivo geometry

MULTIFOCAL CEREBRAL GAS EMBOLISM (CGE) is a known risk of cardiac operations and a recognized hazard of diving decompression (11). Some of the most serious consequences associated with diving fall in the category of type II decompression sickness (DCS) and involve neurological dysfunction such as motor, sensory, or mental impairment, convulsions, coma, and death (Ref. 14; Association of Diving Contractors, unpublished observations). The cause of the neurological changes is considered, at least in part, to be the result of a diver's ascent rate to the surface exceeding his ability to maintain inert gas remaining in the tissues in a dissolved state. The gas may come out of solution via nucleation and grow into multiple bubbles that are disseminated throughout the tissue and vasculature. Some of these intravascular bubbles potentially become entrapped in the arterial cerebral circulation and cause the local transient ischemia responsible for the diver's neurological impairment (11).

Regardless of the cause, the primary treatment modality for CGE is hyperbaric therapy (HT) (11). This treatment consists of initially "recompressing" the patient to an elevated external pressure and usually includes providing a specialized breathing mixture. This breathing mixture can contain one of several gas combinations, air, nitrox (an N_2-O_2 mixture), or heliox (an He-O_2 mixture), as well as a variable percentage of inert gas (79, 67.5, or 50%), with O_2 providing the balance. The ambient pressure and breathing mixtures are subsequently changed over time in a stepwise fashion to return the patient to atmospheric pressure and air breathing with minimal trauma.

The HT protocol depends on the symptoms presented, the depth and length of the dive, and available facilities; however, experiments to define the limits of recompression and variable O_2 treatment are not carried out in humans suffering from DCS. Protocols have been established based on large numbers of clinical experiences with individual cases in naval and industrial organizations. A mathematical model defining the impact of increased levels of external pressure and inhaled O_2 content would, therefore, be very useful in understanding and elucidating potentially beneficial treatment combinations.

Some of the most recognized mathematical models used for calculating bubble growth or decay have assumed a spherical bubble geometry, even when intravascular gas bubbles are simulated (6, 8). On the basis of our earlier published observations (3) and those of other investigators (7, 13), however, it has been shown that gas emboli do not maintain a spherical shape when entrapped in the vessels. The bubbles initially fill the vessel diameter and elongate axially, taking on a "sausage-like" appearance. Using this information, we previously developed a generalized mathematical model calculating the absorption times of single bubbles trapped inside the vasculature that is based on their initial in vivo geometry. This model was validated

Address for reprint requests and other correspondence: D. M. Eckmann, Dept. of Anesthesia, University of Pennsylvania, 7 Dulles/HUP, 3,400 Spruce St., Philadelphia, PA 19104 (E-mail: deckmann@mail.med.upenn.edu).

The costs of publication of this article were defrayed in part by the payment of page charges. The article must therefore be hereby marked "*advertisement*" in accordance with 18 U.S.C. Section 1734 solely to indicate this fact.

through microvascular experiments under ambient conditions and predicted actual absorption times in the intact rat cremaster circulation more accurately than the models in which a spherical configuration was assumed (3).

The goal of this study is to apply our earlier model, by use of a realistic intravascular bubble geometry, to the situation of hyperbaria. This work is a natural extension of our earlier methods and provides the opportunity to manipulate parameters such as external pressure and breathing gas to examine their effects on intravascular bubble absorption dynamics. The importance of this work lies in the fact that this is the first attempt to describe how hyperbaria changes the normal absorption process of CBEs as they appear in vivo.

MATERIALS AND METHODS

Model. The theoretical model we developed to calculate absorption times of a CGE has been described in detail previously (3) but is mentioned very briefly below. We have modeled the in vivo shape of a cerebrovascular bubble as a cylinder of initial length L_o, with hemispherical end caps of initial radius R_o (Fig. 1). On the basis of in vivo findings, we stipulate that, as gas absorbs out of the bubble, the cylindrical portion of the embolism decreases in length while the radius of the hemispherical end caps remains fixed. Once the cylindrical portion completely disappears, the remaining hemispherical end caps fuse together to form a sphere. This spherical geometry is maintained for the remainder of the bubble absorption. The absorption of the bubble can, therefore, be solved independently for two separate phases in time, the cylindrical phase and the spherical phase, in each case with the use of Fick's law for the specific bubble geometry. The time for the bubble to absorb is highly dependent on the initial aspect ratio of the bubble itself, or L_o/R_o.

During each phase of bubble absorption, the expression for the pressure inside the bubble is based on several simplifying assumptions. We assume that there is rapid equilibrium of the metabolic gases (O_2, CO_2, and water vapor) between the inside of the bubble and the tissue, with constant tissue partial pressure of these gases maintained. The initial rapid efflux of the inert gas at the time of entrapment is neglected, and capillary perfusion from surrounding vessels is postulated to carry the excess gas away from the bubble interface. The hydrostatic head of blood pressure on the bubble is assumed to be small compared with the external barometric pressure and is, therefore, ignored. The elastic force exerted on the bubble by the vessel wall is also neglected, inasmuch as any change in vessel diameter would merely cause the bubble to lengthen or shorten, without an increase or decrease in internal pressure. The pressure inside the bubble is balanced only by a surface tension term proportional to the inverse of the bubble radius and the difference between the external pressure acting on the bubble and the partial pressures of O_2, CO_2, and water vapor in the tissue. The internal bubble pressure, therefore, remains fixed during the cylindrical portion of absorption due to a constant value of R_o and increases during the spherical phase as the bubble volume and, consequently, the radius decrease.

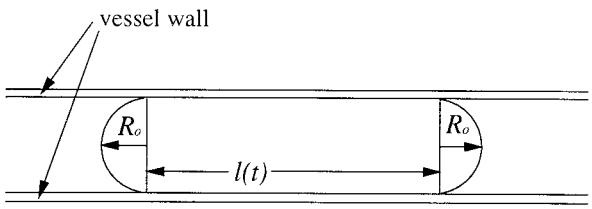

Fig. 1. Model of in vivo gas embolism geometry before the cylindrical core has disappeared. R_o, initial radius; $l(t)$, time-dependent length of cylindrical core.

The time for bubble absorption is readily obtained numerically. With this model, we can calculate the absorption time of an intravascular bubble over a range of geometries for any given initial volume, at any recompression pressure, and for any gas content in the breathing mixture. Knowing local tissue characteristics allows further application to specific areas such as the brain.

Multigas model. The situation in which a diver is breathing one gas mixture during a dive and decompression and another gas mixture during HT becomes more complicated. A CGE that forms during or after the diver surfaces is composed of the inert gas inhaled during the dive and decompression, inasmuch as this is the gas present in the tissues at the time of bubble nucleation and growth. This gas inside the bubble will follow its concentration gradient, diffusing out of the bubble after the diver surfaces. Introducing a second inert gas in the inhaled breathing mixture during recompression loads the tissues and arterial blood with a new gas species heretofore not present inside the bubble. While the gas inside the bubble diffuses outward, the new gas present in the tissues follows its concentration gradient, diffusing into the bubble. The net effect of gases moving into and out of the bubble can be to slow absorption or even promote bubble growth. To describe this more complex situation, we developed the in vivo multiple gas model based on the same bubble geometry as described above and the basic assumptions defined by Burkard and Van Liew (4).

Our multiple gas model was validated by simulating conditions of only one gas and comparing results with those obtained from the single gas model for a given bubble volume and geometry. In all cases, the absorption times calculated using any of the models never differed by >2.0%.

Simulations. We examined three groups of DCS treatments: hyperbaric simulations with air, hyperbaric simulations with variable O_2, and multigas simulations. The simulations were applied to the specific case of a cerebrovascular bubble, since arterial emboli in the cerebral circulation are assumed to be responsible for the most serious consequences associated with DCS (11). A single representative bubble was used for simplicity, albeit DCS is usually characterized by multiple gas emboli distributed throughout the vasculature and tissues. A bubble, initially 50 nl in volume at ambient pressure, was simulated, because this embolism size is a reasonable estimate based on physiological bubbles seen by Powell and Weydig (13) in the microcirculation of adipose tissue of rats and rabbits exposed to rapid decompression.

We assumed that all divers maintained a constant body temperature of 37°C during treatment. The appropriate physiological parameters for cerebral tissue were found in the literature (4, 6, 18) or estimated on the basis of available information and are presented in Table 1.

To model the different initial steps of various recompression protocols, we varied the external pressure on the patient and calculated the partial pressure of the gas in the arterial blood on the basis of the percentage in the inspired breathing mixture during recompression. The partial pressure of the inert gas in the arterial blood is relevant to our model, because on the basis of our unpublished observations, a 50-nl arterial gas bubble typically lodges in a 100- to 200-μm-diameter arteriole. The increase in external pressure due to

Table 1. *Physiological values of mathematical variables used to calculate cerebral gas embolism absorption dynamics*

Definition	Variable	Value	Units
Solubility of inert gas *i* in cerebral tissue	$\alpha_{ti(N_2)}$	2.092×10^{-5}	ml·cm^3 brain^{-1}·mmHg^{-1}
	$\alpha_{ti(He)}$	1.375×10^{-5}	ml·cm^3 brain^{-1}·mmHg^{-1}
Solubility of *i* in blood	$\alpha_{b(N_2)}$	1.855×10^{-5}	ml·cm^3 blood^{-1}·mmHg^{-1}
	$\alpha_{b(He)}$	1.229×10^{-5}	ml·cm^3 blood^{-1}·mmHg^{-1}
Diffusivity of *i* in cerebral tissue	D_{N_2}	6.22×10^{-4}	cm^2/min
	D_{He}	1.65×10^{-3}	cm^2/min
External ambient total pressure	P_s	(760 mmHg/atm)·(Y atm)	mmHg
Partial pressure of *i* in arterial blood	Pa_i	$(P_s - Pti_{H_2O})$·(inert gas %)/100	mmHg
Partial pressure of O_2 in cerebral tissue	Pti_{O_2}	Depends on P_s, range 42.8–59.3 (higher for 32.5 and 50% O_2 mixtures)	mmHg
Partial pressure of CO_2 in cerebral tissue	Pti_{CO_2}	Depends on P_s, range 45.8–47.3	mmHg
Water vapor pressure	Pti_{H_2O}	47	mmHg
Surface tension at blood-air interface	σ	0.03545	mmHg/cm
Brain density	y	1.05	g brain/ml brain
Regional cerebral blood flow	$\dot{q}$	0.5	ml blood·cm^3 brain^{-1}·min^{-1}

See Ref. 5 for mathematical details.

undersea diving causes changes in the tissue partial pressures of O_2 and CO_2, which were also accounted for in the models (18).

Hyperbaric simulations with air. We compared the absorption time of a 50-nl bubble left untreated at an external pressure of 1 atmosphere absolute (ATA) with a bubble of the same volume recompressed to pressures of 2.8, 4, and 6 ATA. We selected these values of hyperbaric pressure for our simulations, because the Association of Diving Contractors recommends recompression to 2.8 ATA or 60 feet of seawater (fsw) (Association of Diving Contractors, unpublished observations) for simple DCS symptoms such as limb pain or skin rash, without any accompanying neurological deficit. If, however, there are any signs of type II DCS, the US Navy Diving Treatment Table 6A (16) prescribes an immediate compression to 6 ATA or 165 fsw. To demonstrate the theoretical effects of an intermediate external pressure, we selected 4 ATA, a pressure shown by Waite et al. (19) to be sufficient to cause the disappearance of all cerebrovascular emboli in physiological experiments with dogs breathing air. All simulations used 79% N_2-21% O_2 as the breathing mixture during therapy.

Hyperbaric simulations with variable O_2. To demonstrate the efficacy of accelerating bubble absorption with use of increased concentrations of O_2 in the breathing mixtures during HT, we compared the absorption times of a 50-nl bubble on the surface recompressed to 2.8, 4, and 6 ATA in a patient breathing 21% O_2-79% N_2 (air), 32.5% O_2-67.5% N_2, and 50% O_2-50% N_2. All three of these breathing mixtures are used clinically to treat DCS, depending on the situation presented. The US Navy and Royal Navy Diving Manuals define a treatment for type II DCS that begins with an initial recompression to 6 ATA; however, the US Navy generally supports using 79% N_2-21% O_2 as the breathing gas, whereas the Royal Navy recommends 67.5% N_2-32.5% O_2 (11, 16). A 50% O_2-50% N_2 breathing mixture is endorsed by the Association of Diving Contractors during the initial step of recompression to 6 ATA, but only in cases when a diver with serious DCS has surfaced from an air dive shallower than 6 ATA (unpublished observations).

Multigas simulations. The multigas simulations use the multiple gas model to calculate the time rate of change of the bubble volume for a 50-nl CGE at ambient conditions under an applied external pressure of 6 ATA. The recompressed bubble was given a fixed L_o/R_o of 2.6, inasmuch as this bubble configuration was shown to give the longest absorption times (i.e., representative of the worst-case scenario) at a given bubble volume (3). Heliox, an He-O_2 mixture, is a breathing gas used primarily by commercial and military divers (2); therefore, the multigas simulations were run using heliox (21% O_2-79% He) and air (21% O_2-79% N_2). The model was used to simulate events for the four possible combinations stemming from use of these two inert gases during the two phases of the diving and decompression-recompression: N_2O_2-N_2O_2, HeO_2-HeO_2, N_2O_2-HeO_2, and HeO_2-N_2O_2.

In all the hyperbaric therapies simulated, regardless of the breathing mixture, we predicted that the total time a recompressed 50-nl bubble would take to absorb was ≤30 min. The US Navy and Royal Navy recompression protocols require that the diver spend ≥25–30 min at the initial hyperbaric pressure of 6 ATA; therefore, simulating the initial step of HT is sufficient to model complete embolism absorption into the bloodstream.

RESULTS

The time rate of change of bubble volume during absorption for a 50-nl CBE left untreated in a patient breathing air at ambient pressure is depicted in Fig. 2 for two configurations: a spherical bubble ($L_o/R_o = 0$) and a bubble with L_o/R_o of 2.6. These two values for L_o/R_o were found to give the minimum and maximum absorption time, respectively, for a bubble of a given volume (3). The model predicts that a spherical bubble with an initial radius of 228 μm would take 177 min to absorb, whereas a bubble of the same volume with an initial radius of 159 μm and an initial central core length of 414 μm would take 296 min to absorb (Fig. 2). The maximum absorption time for a 50-nl bubble is, therefore, 67% longer than if the bubble were to remain a sphere. The discontinuity in the volume vs. time curve for the embolism with L_o/R_o of 2.6 represents the transition from the cylindrical to the spherical absorption phase, as discussed elsewhere (3).

Hyperbaric simulations with air. We used our model to calculate the theoretical absorption times of an air bubble, initially 50 nl at sea level, over a range of

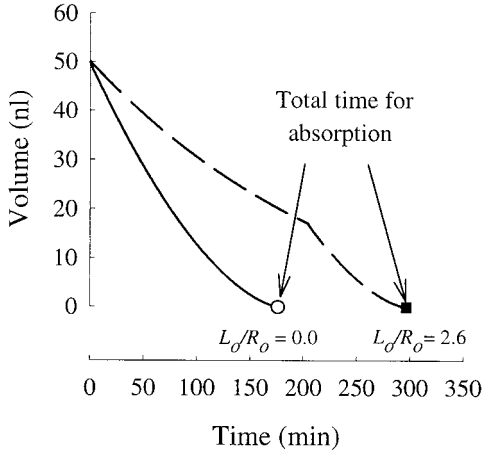

Fig. 2. Bubble volume over time for a 50-nl cerebral gas embolism at ambient pressure and 2 distinct aspect ratios (L_o/R_o): a spherical bubble (L_o/R_o = 0.0, solid line) and L_o/R_o = 2.6 (dashed line). ○, Total time required for absorption of a spherical bubble; ■, absorption time for the same bubble volume with L_o/R_o = 2.6.

geometries at several different hyperbaric pressures. Because embolism absorption time is clearly dependent on L_o/R_o and, hence, initial bubble geometry (Fig. 2), we plotted the total time for bubble absorption as a function of initial surface area, corresponding to L_o/R_o between 0 (spherical bubbles) and 25 (long slender bubbles). Each recompression pressure, 2.8, 4, and 6 ATA, generates a unique initial bubble volume; therefore, each curve in Fig. 3 represents a different initial bubble volume over the same range of L_o/R_o values.

The far left side of each of the curves in Fig. 3 represents the minimum surface area for a given volume (i.e., a sphere). In the untreated case, 1 ATA, the absorption time on the far left of the curve, corresponds to 180 min, calculated by a slightly different method but approximately equal to the total time for absorption of a spherical bubble shown in Fig. 2. A maximum absorption time also exists for each recompression curve, at L_o/R_o of ~2.6. Again there is agreement between the maximum value on the untreated curve in Fig. 3, 298 min, and the total time for absorption of a bubble with L_o/R_o of 2.6 (Fig. 2).

Subjecting a patient with a 50-nl CGE at ambient conditions (in which bubble growth due to decompression is no longer occurring) to 6 ATA recompression therapy is calculated to reduce the maximum possible absorption time from 298 min in the untreated case to 7.5 min, a reduction of 98%. The decrease in bubble absorption time, however, is not a linear function of the external pressure (Fig. 3). A step change from 1 to 2.8 ATA corresponds to a decrease in the maximum absorption time from 298 to 30 min or 90%, while a change from 1 to 4 ATA reduces the maximum absorption time to 16 min, a decrease of 95%.

Hyperbaric simulations with variable O_2. The effects of changing the inert gas content in the inspired breathing mixture are shown in Fig. 4. The range of absorption times theoretically possible for a gas bubble, originally 50 nl at ambient conditions, is presented as a function of hyperbaric pressure for various concentrations of O_2 in the breathing mixture during recompression: 21% O_2-79% N_2, 32.5% O_2-67.5% N_2, and 50% O_2-50% N_2. Decreasing the N_2 content of the inspired gas from 79% to 67.5% was calculated to reduce the maximum absorption time of a bubble at 2.8 ATA by ≥40%, from 30 to 18 min. An even greater reduction in maximum absorption time was achieved when the breathing mixture contained 50% O_2 instead of 21% O_2, changing the maximum CGE residence time from 30 to 11 min, a decrease of 63%. The relative percent reduction in maximum absorption time between the various breathing gases was consistent at all the recompression pressures, 2.8, 4, and 6 ATA.

The decrease in bubble volume associated with each hyperbaric pressure is shown in Fig. 4*B*. An increase in the external pressure from 1 to 2.8 ATA reduces a 50-nl bubble to 15.6 nl. If this same bubble is exposed to 6 ATA, the bubble volume is compressed to 6.9 nl, a reduction of 43.1 nl from the untreated size. A slight variation (≤1.3 nl) in the recompressed bubble volume exists between the different breathing gases at the same hyperbaric pressure. This occurs because the internal bubble pressure is dependent on the partial pressure of O_2 in the tissue, in equilibrium with the

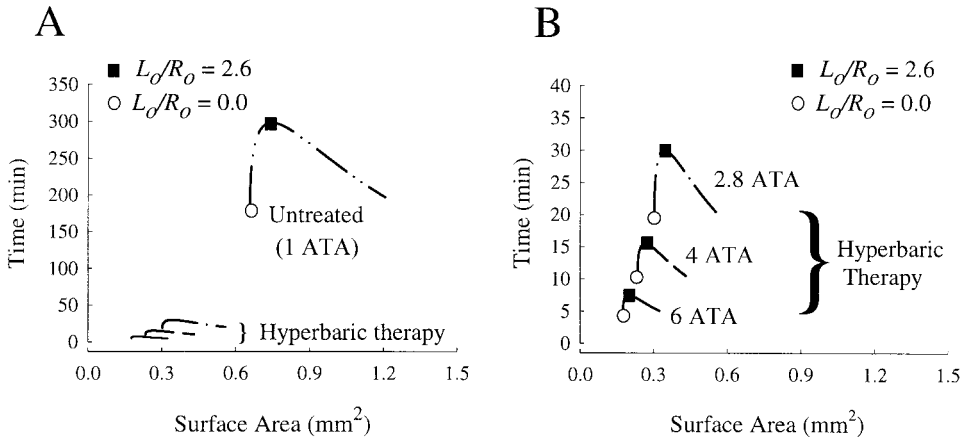

Fig. 3. Predicted absorption times for an embolism recompressed to several hyperbaric pressures over a range of initial bubble geometries. All curves are for an initially uncompressed bubble volume of 50 nl. *A*: pressure conditions are as follows: untreated bubble (dashed line with 2 dots), 2.8 ATA (dashed line with 1 dot), 4 ATA (dashed line), and 6 ATA (solid line). *B*: enlarged view of the 3 pressures representing hyperbaric therapy.

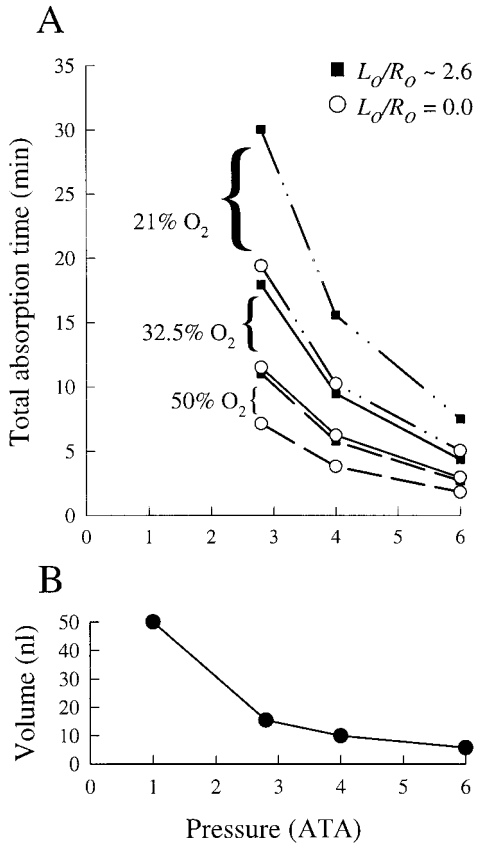

Fig. 4. *A*: calculated absorption times for a 50-nl cerebrovascular bubble (before recompression) at various hyperbaric pressures. Lines define the range of possible absorption times for conditions of inspired O_2 concentration as follows: 21% (dashed line with 2 dots), 32.5% (solid line), and 50% (dashed line). Balance gas is N_2. ○, Absorption time for a spherical bubble; ■, maximum possible absorption time. *B*: resultant compressed bubble volume of a cerebral gas embolism originally 50 nl at ambient pressure at various hyperbaric pressures.

bubble, which is obviously related to the concentration of O_2 in the breathing gas.

At specific pressures, the curves representing the maximum and minimum residence times for a cerebrovascular bubble in a patient breathing each of the gas mixtures do not overlap with one another at any point in Fig. 4, regardless of the recompression pressure evaluated. The lack of overlap indicates that even the longest possible absorption time for a CGE with 32.5% O_2 in the breathing mixture at a given pressure is still ≥4% more rapid than the shortest possible absorption time in a patient breathing 21% O_2. Likewise, the same-size CGE in a patient breathing 50% O_2 absorbs a minimum of 5% faster and a maximum of 37% faster than if the patient were breathing 32.5% O_2.

Multigas simulations. The step change in bubble volume, as a result of the initial recompression from sea level to 6 ATA, is from 50 nl at ambient pressure to 6.9 nl. The subsequent changes in bubble volume over time during HT at 6 ATA for four different diving and decompression-recompression gas variations are shown in Fig. 5. The shortest absorption time predicted for any of the combinations was 4.4 min, in the case of an individual breathing He continually during the dive, decompression, and recompression therapy (HeO_2-HeO_2). Changing the recompression breathing mixture to N_2 instead of He (the HeO_2-N_2O_2 case) increased bubble absorption time by only ~3%. However, although overall absorption time was slightly longer in the HeO_2-N_2O_2 than in the HeO_2-HeO_2 case, bubble absorption was actually accelerated for a majority of time, as indicated by a smaller bubble volume at any given time. When the bubble was formed by breathing N_2 during diving and decompression, regardless of the gas inhaled during recompression, however, absorption times increased dramatically, by 49% in the N_2O_2-HeO_2 case and by 73% with N_2O_2-N_2O_2. The multigas combination of a bubble initially composed of N_2 and absorbing in the presence of He was the only case that showed even a temporary increase in bubble volume, although the absorption time, 6.5 min, was still predicted to be less than in the N_2O_2-N_2O_2 case of 7.6 min.

To determine the relationship between the behavior of the individual gases as they relate to the dynamics of the total bubble volume, we tracked the influx and efflux of the two individual gases, along with the resultant bubble volume. The time rate of change of bubble volume for the two cases in Fig. 5 involving multiple gases (HeO_2-N_2O_2 and N_2O_2-HeO_2) is graphed in Fig. 6. The bubble initially composed of He and exposed to N_2 during recompression takes a total of 4.5 min to absorb; however, all the He has diffused out of the bubble by 3.5 min. The initial influx of N_2, therefore, slows bubble absorption slightly but not to the point of causing bubble growth or proving to be disadvantageous compared with the HeO_2-HeO_2 case.

The theoretical prediction for the opposing case, a patient with a CGE initially containing only the inert

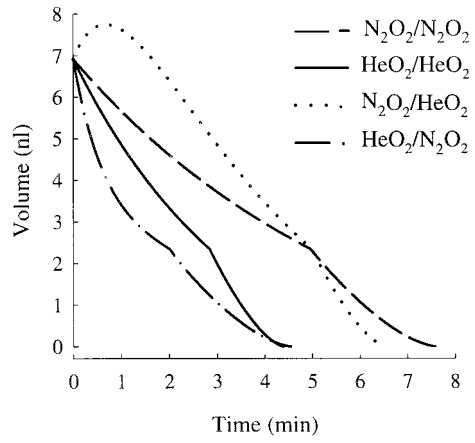

Fig. 5. Time history of bubble volume predicted for different combinations of diving and recompression breathing gas mixtures. All curves are for a 50-nl bubble recompressed to 6 ATA with L_o/R_o = 2.6. Breathing gas mixtures are as follows: 79% N_2-21% O_2 during diving, decompression, and recompression (dashed line), 79% He-21% O_2 during diving, decompression, and recompression (solid line), 79% N_2-21% O_2 during diving and decompression and 79% He-21% O_2 during recompression (dotted line), and 79% He-21% O_2 during diving and decompression and 79% N_2-21% O_2 during recompression (dashed-dotted line).

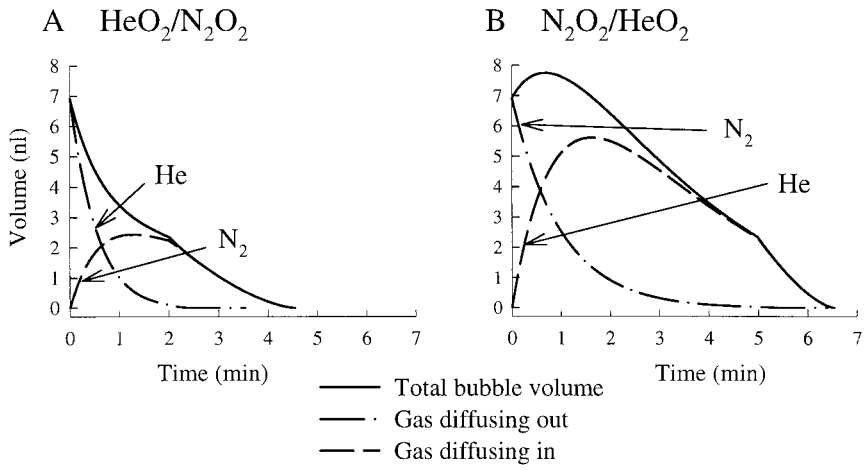

Fig. 6. Influx and efflux of the inert diving and recompression gases, along with the resultant total bubble volume over time, for 2 cases involving multiple inert gases. L_o/R_o is set to 2.6 for a 50-nl ambient bubble, recompressed to 6 atm. In both cases, HeO_2-N_2O_2 and N_2O_2-HeO_2, curves represent total bubble volume (solid line), gas breathed during diving and decompression, diffusing out of the bubble (dashed-dotted line), and gas inhaled during recompression, diffusing into the bubble (dashed line). *A*: gas exchange for a cerebral gas embolism in the case of a diver breathing HeO_2 during the dive and decompression and N_2O_2 during recompression. *B*: individual gas components in an embolism of a diver breathing N_2O_2 during diving and decompression and HeO_2 during hyperbaric therapy.

gas N_2 and breathing He-O_2 during recompression, takes 2 min longer to absorb. The CGE grows in volume for the first 41 s, demonstrating that the rapid influx of He into the bubble exceeds the rate at which N_2 diffuses out. The recompression gas, He, reaches a maximum volume inside the bubble of 5.6 nl, whereas in the HeO_2-N_2O_2 case, N_2 peaks at only 2.4 nl in the bubble.

DISCUSSION

In the absence of the ability to assess the most effective treatment options available with HT clinically, a mathematical model was used to predict the residence time of a gas embolism as a function of specific bubble geometry (Fig. 1) and various treatment parameters. An entrapped 50-nl embolism left untreated in the cerebral circulation is predicted to have absorption times of ~177 to 296 ± 2 min depending on the configuration (Fig. 2) and the model used. As shown in Fig. 3, the residence time of a cerebrovascular bubble is a nonlinear function of initial surface area, demonstrating competing mechanisms for bubble absorption. Increasing the bubble surface area, through bubble elongation and narrowing, creates a larger area for gas diffusion out of the bubble and is advantageous for absorption; however, this alone does not lead to a decrease in absorption time. An increased surface area also indicates a longer bubble length and, therefore, a greater fraction of bubble volume, which must be absorbed before the cylindrical core disappears and the internal pressure rises. This theoretically inhibits bubble absorption, especially in aspect ratios between 0.3 and 13.1, and has heretofore been overlooked in theoretical models in which a spherical bubble geometry is assumed (3).

To illustrate the theoretical basis behind the clinically proven therapeutic effects of recompression and various inhaled gas mixtures on embolism absorption dynamics, we simulated the conditions of hyperbaria with air and hyperbaria with variable O_2 and multiple gases used to treat patients with DCS with our theoretical model.

Hyperbaric simulations with air. In Fig. 3, a recompression pressure as low as 2.8 ATA is shown to have a dramatic effect on reducing the bubble absorption time, by ~90%. This decrease in the residence time is attributed in part to the large reduction in bubble volume. The large increase in external pressure due to hyperbaria does not change the basic behavior of bubble absorption, however, inasmuch as all the curves presented in Fig. 3 have the same fundamental shape.

Hyperbaric simulations with variable O_2. HT can include a manipulation not only of the external pressure but also of the inhaled breathing mixture. The combination of these therapies demonstrates that lowering the inert gas content in the breathing mixture from 79% to 67.5% or 50% at a given recompression pressure is a viable way to decrease bubble absorption time from 40% to 63% for all pressures (Fig. 4). Reducing the inert gas concentration in the inspired gas mixture is shown to increase the rate of bubble absorption to similar values obtained by increasing the external pressure. The drawbacks associated with this manipulation are not included in the model, however. Theoretically, the optimal breathing mixture at any recompression pressure would be 100% O_2, thereby reducing to zero the inert gas percentage in the breathing mixture and the tissues and maximally accelerating diffusion out of the bubble. The most significant problem associated with this approach is O_2 toxicity, manifested by sudden seizures (5). O_2 toxicity is particularly harmful in previously ischemic tissue, injuring endothelial cells (10, 15). Inhalation of 100% O_2 has proven to be beneficial in the continuation of therapy; however, when the patient is initially subjected to large recompression pressures and a high O_2 content in the breathing mixture, O_2 toxicity becomes an obvious concern. The disadvantage of keeping the O_2 content at 21% is the extensive time required to return the patient to ambient pressure (Ref. 16; Association of Diving Contractors, unpublished observations).

A difference of 1–28 min can be achieved in absorption times by adjusting the recompression pressure and inhalation mixture, a time potentially vital to the

patient's recovery. Any prolongation of bubble absorption is additional time during which cerebral tissue is cut off from blood flow and susceptible to ischemia. The perpetuation of the gas embolism within the vasculature can also cause platelet aggregation, activation of the thromboinflammatory pathways, and damage to the endothelium, all through contact at the gas-blood vessel interface (1, 12, 20). In addition, this model was run only for a representative CGE of 50 nl at ambient pressure. A larger initial bubble volume would also show a larger discrepancy in bubble absorption times.

The model demonstrates the two primary factors, which are manipulated during HT to reduce the residence time of CGE: external pressure and inert gas content of the breathing mixture. Within the limits of these parameters, there is room for considerable adjustment of both. Although a difference of 28 min in CGE absorption time may not appear significant when the total time required to diagnose, transport, and prepare the patient is considered, this difference in time represents a discrepancy between various treatment methods, during which the embolism is made to shrink. During the diagnosis and transport stages, the embolism can be growing in size and numbers, inasmuch as divers can experience an exacerbation of symptoms before treatment (Association of Diving Contractors, unpublished observations). For this reason, prompt initiation of therapy is extremely important, and once treatment has begun, everything possible should be done to reduce the residence time of the embolism. This model can be used in assessing the benefits associated with the possible combinations in recompression therapy and can aid in understanding the relationship between the various aspects involved in the clinical treatment of CGE.

Multigas simulations. To investigate other bubble absorption phenomena, which occur in divers exposed to more than one breathing gas, we incorporated the multiple gas concept, accounting for divers breathing one inert gas during the dive and decompression and another during the recompression therapy. One might initially predict that combinations with different inhalation gases for diving and recompression will absorb most quickly, inasmuch as the tissue concentration of the gas species inside the bubble during recompression would be negligible, thus increasing the gradient that drives absorption out of the bubble. Although this is basically true, counterdiffusion of the new inert gas, introduced in the breathing mixture, into the bubble during recompression effectively slows absorption. The model presented accounts for this important effect.

The counterdiffusion of gas into the bubble is responsible for the initial increase of bubble volume predicted in the multiple gas case, in which a diver inhaling N_2 and O_2 during a dive and presenting with CGEs is recompressed while breathing He and O_2. This same bubble growth does not occur in a gas embolism of a patient diving with He and being recompressed with N_2 (Fig. 5). The results of the simulations also predict that the absorption time of a CGE is actually longest in a diver continually breathing air during the dive, decompression, and recompression, as illustrated in Fig. 5, 61 s longer than if the patient were inhaling He as the inert gas during compression. These results agree with physiological experiments performed by Hyldegaard et al. (9) demonstrating a reduced residence time for bubbles in rats when He was given as the inert breathing mixture instead of N_2 after the animals surfaced from decompression with air. The two emboli initially containing He appear to have distinctly faster absorption than the bubbles initially containing N_2, regardless of the recompression gas inhaled. This is in part due to the high diffusion coefficient of He, which promotes its rapid efflux (Table 1).

To understand the mechanisms behind the bubble absorption dynamics in the multiple gas cases, it becomes necessary to examine total bubble volume as a function of the individual inert gas volumes at any given time (Fig. 6). Of the two initial inert gases in each of the bubbles, He has a much faster rate of absorption into the cerebral tissue than N_2. Similarly, He proves to have the larger rate of diffusion into the bubble from the tissues as well. In combination, these factors dictate that the embolism composed of He and collapsing during a recompression with N_2 will absorb much faster than if the opposing conditions are present. The clinical implications of this prediction are that an embolism appearing in a patient after surfacing from a He dive would reside for a shorter time in a vessel with less likelihood of causing cerebral ischemic injury than if the embolism were created from an air dive. A difference of ~2 min may not be enough to affect clinical treatment, but it may reflect the relation between tissue ischemia and infarction. The model aids in prediction of absorption dynamics when a diver is exposed to multiple gases during decompression-induced gas embolism and therapy and indicates potential for decreasing the bubble residence time.

This model, while helpful in gaining a basic understanding of bubble dynamics in the presence of elevated external pressures and different inhaled gas mixtures, also has limitations. When various aspects of HT are simulated, the manipulations in recompression pressures or breathing gases are modeled as instantaneous step changes to simplify the solution. In reality, it takes ~3–5 min to recompress a patient to 6 ATA, depending on his tolerance, during which time the inert gas in the tissue must also approach equilibrium with the breathing mixture, and this has not been factored into the model. To further simplify the model, we assumed that once a bubble became entrapped in a cerebral vessel at a given initial geometry and hyperbaric pressure, the bubble did not dislodge to a location further downstream with a new aspect ratio, although this has been observed occasionally in vivo (3).

This theoretical model is based on the configuration of a CGE in vivo and demonstrates the various interactions of bubble geometry, recompression pressure, and inhaled gas mixtures taking part in determining the residence time. Manipulating the different parameters individually and in conjunction with one another to simulate events resulting from general practice in

the initial treatment phase of DCS provides a simple and effective method of establishing the relevant factors in determining the absorption time and basic dynamics of CGEs. Once these factors are well understood, the model can be used to predict the limits of current and experimental therapies to reduce the damaging effects of CGE.

Dr. Roderic Eckenhoff provided helpful discussion.

This study was supported by National Heart, Lung, and Blood Institute Grant R01 HL-60230.

REFERENCES

1. **Albertine KH, Wiener-Kronish JP, Koike K, and Staub NC.** Quantification of damage by air emboli to lung microvessels in anesthetized sheep. *J Appl Physiol* 57: 1360–1368, 1984.
2. **Bennett PD.** Inert gas narcosis. In: *The Physiology and Medicine of Diving*, edited by Bennett PD and Elliott DH. San Pedro, CA: Best, 1982, p. 239–261.
3. **Branger AB and Eckmann DM.** Theoretical and experimental intravascular gas embolism absorption dynamics. *J Appl Physiol* 87: 1287–1295, 1999.
4. **Burkard ME and Van Liew HD.** Simulation of exchanges of multiple gases in bubbles in the body. *Respir Physiol* 95: 131–145, 1994.
5. **Clark JJ.** Oxygen toxicity. In: *The Physiology and Medicine of Diving*, edited by Bennett PD and Elliott DH. San Pedro, CA: Best, 1982, p. 201–238.
6. **Dexter F and Hindman BJ.** Recommendations for hyperbaric oxygen therapy of cerebral air embolism based on a mathematical model of bubble absorption. *Anesth Analg* 84: 1203–1207, 1997.
7. **Feinstein SB, Shah PM, Bing RJ, Meerbaum S, Corday E, Chang B-L, Santillan G, and Fujibayashi Y.** Microbubble dynamics visualized in the intact capillary circulation. *J Am Coll Cardiol* 4: 595–600, 1984.
8. **Hlastala MP and Van Liew HD.** Absorption of in vivo inert gas bubbles. *Respir Physiol* 24: 147–158, 1975.
9. **Hyldegaard O, Moller M, and Madsen J.** Effect of He-O_2, O_2, and N_2O-O_2 breathing on injected bubbles in spinal white matter. *Undersea Biomed Res* 18: 361–371, 1991.
10. **Kazzaz JA, Xu J, Palaia TA, Mantell L, Fein AM, and Horowitz S.** Cellular oxygen toxicity: oxidant injury without apoptosis. *J Biol Chem* 271: 15182–15186, 1996.
11. **McDermott JJ, Dutka AJ, Koller WA, and Flynn ET.** Effects of an increased Po_2 during recompression therapy for the treatment of experimental cerebral arterial gas embolism. *Undersea Biomed Res* 19: 403–413, 1992.
12. **Philp RB, Inwood MJ, and Warren BA.** Interactions between gas bubbles and components of the blood: implications in decompression sickness. *Aerospace Med* 43: 946–953, 1972.
13. **Powell MR and Weydig KJ.** *In Vivo Bubble Growth Studies Following Decompression.* Tarrytown, NY: Union Carbide Technical Center, 1974. (Tech Rep CRT-T-798.74)
14. **Reul J, Weis J, Jung A, Willmes K, and Thron A.** Central nervous system lesions and cervical disc herniations in amateur divers. *Lancet* 345: 1403–1405, 1995.
15. **Shinomiya N, Suzuki S, Hashimoto A, Ito N, Takaai Y, and Oiwa H.** Effect of hyperbaric oxygen on intracellular adhesion molecule-1 (ICAM-1) expression in murine lung. *Aviat Space Environ Med* 69: 1–7, 1998.
16. **US Navy.** *US Navy Diving Manual*, revision 4. Washington, DC: GPO, 2000. (Navsea Tech. Manual 5, 21-42).
18. **Van Liew HD, Conkin J, and Burkard ME.** The oxygen window and decompression bubbles: estimates and significance. *Aviat Space Environ Med* 64: 859–865, 1993.
19. **Waite CL, Mazzone WF, Greenwood ME, and Larsen RT.** Dysbaric cerebral air embolism. *Proc 3rd Symp Underwater Physiol 1967*, p. 205–215.
20. **Warren BA, Philp RB, and Inwood MJ.** The ultrastructural morphology of air embolism: platelet adhesion to the interface and endothelial damage. *Br J Exp Pathol* 54: 163–172, 1973.